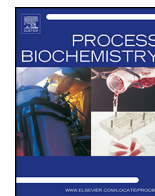




Contents lists available at ScienceDirect

Process Biochemistry

journal homepage: www.elsevier.com/locate/procbio



Isotherm, kinetic and thermodynamic characteristics of adsorption of paclitaxel onto Diaion HP-20

Hong Sik Shin, Jin-Hyun Kim*

Department of Chemical Engineering, Kongju National University, Cheonan 330-717, South Korea

ARTICLE INFO

Article history:

Received 29 December 2015
Received in revised form 11 February 2016
Accepted 21 March 2016
Available online xxx

Keywords:

Paclitaxel
Diaion HP-20
Adsorption isotherm
Kinetics
Thermodynamics

ABSTRACT

Batch experiment studies were carried out on the adsorption of the anticancer agent paclitaxel using Diaion HP-20 while varying parameters such as initial paclitaxel concentration, contact time and adsorption temperature. The experimental data were fitted to the Langmuir, Freundlich, Temkin and Dubinin-Radushkevich isotherm models. Comparison of results revealed that the Langmuir isotherm model could account for the adsorption isotherm data with the highest accuracy among the four isotherm models considered. From the analysis of adsorption isotherms, it was found that adsorption capacity increased with increasing temperature and the adsorption of paclitaxel onto HP-20 was favorable and process could be physical in nature. The obtained kinetics data for paclitaxel adsorption onto HP-20 agreed well with the pseudo-second-order model, and intraparticle diffusion played a dominated role in paclitaxel adsorption according to the intraparticle diffusion model. Thermodynamic parameters, such as standard enthalpy (ΔH°), standard entropy (ΔS°) and standard Gibbs free energy (ΔG°) change, were investigated. The results indicated that the process of paclitaxel adsorption onto HP-20 was endothermic, irreversible, spontaneous and by hydrophobic interaction.

© 2016 Elsevier Ltd. All rights reserved.

1. Introduction

Paclitaxel (Fig. 1) is a diterpenoid anticancer agent that was discovered in the bark of the yew tree [1]. It has been widely used to treat ovarian, breast, lung, pancreatic and other cancers [2]. The demand for this drug is expected to increase steadily; its indications, which include rheumatoid arthritis and Alzheimer's disease, are expanding continuously, and clinical trials for combined prescription with other therapies are being conducted [3,4]. The main methods of paclitaxel production are direct extraction from the yew tree, semi-synthesis involving the chemical combination of side chains after obtaining precursors (baccatin III, 10-deacetylbaccatin III, 10-deacetylpaclitaxel, etc.) from the leaves of the yew tree, and plant cell culture from the bioreactor after inducing a callus and performing a seed culture [5–7]. Among these methods, plant cell culture has the advantage of mass-producing a certain quantity of paclitaxel because stable production is possible within the bioreactor without being affected by external factors such as climate and environment [6].

Secondary metabolites as potential anticancer agents produced by plant cell culture are generally insoluble in water and contained in plant cells [2,8]. In the production of paclitaxel by plant cell cultures of *Taxus chinensis*, most of the paclitaxel is found in plant cells or cell debris and the small amount of water-soluble paclitaxel is found in the culture supernatant. The concentration of paclitaxel dissolved in the culture supernatant is limited and therefore the content of paclitaxel in the culture supernatant relatively decreases as the production quantity increases. In other words, as the production of paclitaxel increases in the bioreactor, the quantity of paclitaxel obtained from plant cells recovered by centrifuge increases and the quantity of paclitaxel in the culture supernatant decreases [9]. However, if the production of paclitaxel decreases in the bioreactor, the quantity of paclitaxel in the culture supernatant relatively increases. For example, if the concentration of paclitaxel produced by plant cell culture in the bioreactor is 20 mg/L, the portion of the paclitaxel remained in the culture supernatant after centrifugation is about 20% or more [2]. In this case, it is very important to perfectly recover paclitaxel from the culture supernatant in terms of overall yield.

Kim and Hong [9] in 2000 first reported how to recover paclitaxel in the culture supernatant and it could be recovered effectively by an adsorption process. In particular, a macroporous synthetic adsorbent, Diaion HP-20 (styrene, highly porous polymer)

* Corresponding author.

E-mail address: jinhyun@kongju.ac.kr (J.-H. Kim).

Nomenclature

B	Temkin constant related to heat of sorption (J/mol)
b_T	Temkin isotherm constant
C	Boundary layer thickness
C_0	Liquid-phase initial concentration of paclitaxel (mg/L)
C_e	Liquid-phase equilibrium concentration of paclitaxel (mg/L)
C_t	Liquid-phase concentration of paclitaxel at time t (mg/L)
E	Adsorption energy (kJ/mol)
ΔG°	Standard Gibbs free energy change (kJ/mol)
ΔH°	Standard enthalpy change (kJ/mol)
ΔH_x	Isosteric heat of adsorption (kJ/mol)
K_{DR}	Mean free energy of sorption per molecule of sorbate (mol^2/J^2)
K_F	Freundlich constant related to adsorption capacity ($\text{mg/g} (\text{L/mg})^{1/n}$)
k_1	Pseudo-first-order rate constant (h^{-1})
k_2	Pseudo-second-order rate constant (g/mg h)
k_i	Intraparticle diffusion rate constant ($\text{mg/g h}^{1/2}$)
k_{i1}	Intraparticle diffusion rate constant at stage I ($\text{mg/g h}^{1/2}$)
k_{i2}	Intraparticle diffusion rate constant at stage II ($\text{mg/g h}^{1/2}$)
K_L	Langmuir constant related to rate of adsorption (L/mg)
K_T	Temkin equilibrium binding constant (L/g)
N	Number of data points
$1/n$	Heterogeneity factor
n	Freundlich constant related to adsorption intensity
q_{cal}	Calculated adsorption capacity (mg/g)
q_D	Theoretical isotherm saturation capacity (mg/g)
q_e	Amount of adsorbate adsorbed per unit mass of adsorbent at equilibrium (mg/g)
q_{exp}	Experimental adsorption capacity (mg/g)
q_{max}	Langmuir constant related to maximum adsorption capacity (mg/g)
q_t	Amount of paclitaxel adsorbed per unit mass of adsorbent at time t (mg/g)
Δq	Normalized standard deviation (%)
R	Gas constant (8.314 J/mol K)
R_L	Dimensionless equilibrium parameter
r^2	Coefficient of determination
ΔS°	Standard entropy change (kJ/mol K)
T	Absolute temperature (K)
V	Volume of solution (L)
W	Mass of adsorbent used (g)

Greek letters

ε Dubinin-Radushkevich constant

Notes

$^\circ$ As a superscript, denotes the standard state
 Δ Difference operator

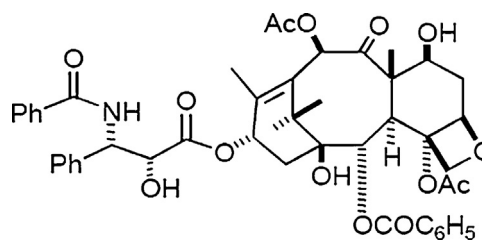


Fig. 1. The chemical structure of paclitaxel.

dynamics. It is important to understand the feasibility and nature of the adsorption process. Therefore, we systematically investigated the characteristics of the adsorption of paclitaxel onto HP-20 for recovery of paclitaxel from the culture supernatant in terms of adsorption isotherms, kinetics and thermodynamics and provided useful information on the adsorption process. The experimental data for paclitaxel adsorbed onto HP-20 were compared using four isotherm equations, namely, Langmuir, Freundlich, Temkin and Dubinin-Radushkevich, to select the best adsorption isotherm that could represent the experimental data. These adsorption isotherms were also used to investigate the trend of adsorption and the characteristics and applicability of the adsorption process. To investigate the mechanisms of paclitaxel adsorption, characteristic constants of adsorption were determined using three adsorption kinetics models: pseudo-first-order kinetic, pseudo-second-order kinetic and intraparticle diffusion models, and then compared. In addition, thermodynamic parameters such as standard Gibbs free energy change, standard enthalpy change and standard entropy change were investigated to evaluate the feasibility and nature of the adsorption process.

2. Materials and methods**2.1. Plant materials**

A suspension of cells originating from *T. chinensis* was maintained in darkness at 24 °C with shaking at 150 rpm. The cells were cultured in modified Gamborg's B5 medium [10] supplemented with 30 g/L sucrose, 10 mM naphthalene acetic acid, 0.2 mM 6-benzylaminopurine, 1 g/L casein hydrolysate, and 1 g/L 2-(*N*-morpholino)ethanesulfonic acid. The cell cultures were transferred to fresh medium every 2 weeks. During prolonged culture for production purposes, 4 mM AgNO₃ was added at the initiation of the culture as an elicitor, and maltose (1 and 2%, w/v) was added to the medium on day 7 and 21, respectively [6]. Following cultivation, plant cells were separated from culture broth using a decanter (CA150 Clarifying Decanter; Westfalia) and high-speed centrifuge (BTPX 205GD-35CDEFP; Alfa-Laval). The culture broth obtained from centrifugation was used in the experiment after filtration through a filter paper (pore size: 2.5 μm). The industrial sample for this study was provided by the Samyang Genex Company, South Korea.

2.2. Paclitaxel analysis

Paclitaxel content was analyzed using a HPLC system (Waters, USA) equipped with a Capcell Pak C18 column (250 mm × 4.6 mm; Shiseido). The elution was performed based on a gradient using a distilled water-acetonitrile mixture varying from 65:35 to 35:65 within 40 min (flow rate = 1.0 mL/min). The injection volume was 20 μL, and the effluent was monitored at 227 nm using a UV detector. Authentic paclitaxel (purity: 97%) was purchased from Sigma-Aldrich and used as the standard [11]. Each sample was analyzed in triplicate.

is inexpensive and effective in the adsorption and desorption of paclitaxel. From an economic point of view, it was the most suitable adsorbent for recovery of paclitaxel in the culture supernatant. However, most previous studies on adsorption have been focused on the optimization of the experimental conditions or process factors and qualitative description of their effects, and very few on the quantitative analysis of adsorption isotherm, kinetics, and thermo-

2.3. Batch studies for adsorption isotherm

Batch studies were performed to investigate the adsorption of paclitaxel from an aqueous solution of culture broth. A predetermined amount of Diaion HP-20 (Mitsubishi Chemical Co., Japan) (0.1 g/L) was added to a 100 mL solution of known paclitaxel concentration (1.6–10 mg/L) in 250-mL Erlenmeyer flasks at various temperatures (25, 30, 35 °C) and agitated at 150 rpm on a thermostatic bath (EYELA, PS-1000) for 24 h. The particle size, surface area, and average pore diameter of HP-20 are 0.3–1.25 mm, 600–650 m²/g, and 24–26 nm, respectively [12]. At predetermined time intervals, the adsorbent was separated by filtration. The content of paclitaxel in the solution was quantitatively analyzed by HPLC. The amount of paclitaxel adsorbed onto HP-20 at equilibrium, q_e (mg/g), was calculated using Eq. (1):

$$q_e = \frac{(C_e - C_0)V}{w} \quad (1)$$

where C_0 and C_e (mg/L) are the concentrations of paclitaxel initially and at equilibrium, respectively, V (L) is the solution volume and W (g) is the weight of adsorbent used.

The adsorption isotherms have been used to describe the equilibrium characteristics of adsorption in order to design the adsorption system and evaluate the applicability of the adsorption process [13]. In this study, the four most common isotherms, namely the Langmuir, Freundlich, Temkin and Dubinin-Radushkevich isotherms, were applied to analyze the adsorption equilibrium experimental data.

2.3.1. Langmuir adsorption isotherm

The Langmuir adsorption isotherm assumes that adsorption occurs at specific homogeneous sites within the adsorbent and the capacity of the adsorbent is finite [13,14]. The linear form of the Langmuir isotherm is given by Eq. (2):

$$\frac{1}{q_e} = \frac{1}{q_{\max}K_L} \frac{1}{C_e} + \frac{1}{q_{\max}} \quad (2)$$

where q_{\max} (mg/g) is the maximum adsorption capacity and K_L (L/mg) is the Langmuir constant related to the energy of adsorption.

2.3.2. Freundlich adsorption isotherm

The Freundlich adsorption isotherm is an empirical equation employed to describe heterogeneous systems. It is based on the assumption of a heterogeneous surface with interaction between adsorbed molecules and a non-uniform distribution of adsorption heat over the surface [14]. The linear form of the Langmuir isotherm is given by Eq. (3):

$$\log q_e = \log K_F + \left(\frac{1}{n}\right) \log C_e \quad (3)$$

where K_F (mg/g[L/mg]^{1/n}) and n are Freundlich isotherm constants that correspond to adsorption capacity and adsorption intensity, respectively.

2.3.3. Temkin adsorption isotherm

The Temkin adsorption isotherm is based on the assumption that the heat of adsorption decreases linearly with the coverage due to the interaction between adsorbate and adsorbent [15]. The linear form of the Temkin adsorption isotherm is generally expressed as Eq. (4):

$$q_e = B \ln K_T + B \ln C_e \quad (4)$$

where B (RT/b_T , J/mol) is a constant related to the heat of adsorption, b_T is a Temkin isotherm constant, R (8.314 J/mol K) is the gas constant, T (K) is the absolute temperature, and K_T (L/g) is the Temkin

isotherm equilibrium binding constant related to maximum binding energy.

2.3.4. Dubinin-Radushkevich adsorption isotherm

The Dubinin-Radushkevich adsorption isotherm is generally applied to express the adsorption mechanism with a Gaussian energy distribution onto a heterogeneous surface [16,17]. The linear form of the isotherm can be expressed as Eq. (5):

$$\ln q_e = \ln q_D - K_{DR} \times \varepsilon^2 \quad (5)$$

where q_D (mg/g) is the theoretical isotherm saturation capacity, K_{DR} (mol²/J²) is the Dubinin-Radushkevich isotherm constant related to the mean free energy of adsorption per mole of the adsorbate, and ε is the Polanyi potential, which is related to the equilibrium as follows:

$$\varepsilon = RT \ln \left[1 + \frac{1}{C_e} \right] \quad (6)$$

The mean energy of adsorption energy, E (kJ/mol) can be calculated using Eq. (7).

$$E = \frac{1}{\sqrt{2K_{DR}}} \quad (7)$$

2.4. Batch studies for adsorption kinetics

Zero-point-one grams per liter of the adsorbent HP-20 was added to a 100 mL solution with an initial paclitaxel concentration of 5.7 mg/L in 250-mL Erlenmeyer flasks at 25 °C and agitated at 150 rpm on a thermostatic bath (EYELA, PS-1000) for 0.5, 1, 3, 6, 12, 24, 30 and 48 h. The temperature for adsorption kinetics, 25 °C, was determined by considering the actual industrial operating temperature [9]. The samples were separated by filtration at predetermined time intervals and analyzed quantitatively by HPLC. The amount of adsorption was calculated by Eq. (8):

$$q_t = \frac{(C_0 - C_t)V}{W} \quad (8)$$

where C_0 and C_t (mg/mL) are the concentrations of paclitaxel initially and at any time t , respectively. The kinetic data were then fitted using the pseudo-first-order, pseudo-second-order and intraparticle diffusion models.

2.4.1. Pseudo-first-order kinetic model

The pseudo-first-order kinetic model was proposed by Lagergren and Svenska [18]. The integrated linear form of this model is expressed as Eq. (9):

$$\ln(q_e - q_t) = \ln q_e - k_1 t \quad (9)$$

where q_e (mg/g) is the amount of paclitaxel adsorbed at equilibrium, q_t (mg/g) is the amount of paclitaxel adsorbed at any time, and k_1 (h⁻¹) is the first-order rate constant.

2.4.2. Pseudo-second-order kinetic model

The linearized form of the pseudo second-order kinetic model can be expressed as Eq. (10) [19]:

$$\frac{t}{q_t} = \frac{1}{k_2 q_e^2} + \frac{1}{q_e} t \quad (10)$$

where k_2 (g/mg h) is the pseudo second-order rate constant.

2.4.3. Intraparticle diffusion model

The intraparticle diffusion model is a theory suggested by Weber and Morris [20] and is used to determine the intraparticle diffusion mechanism. It is applied to most adsorption processes. The

adsorbed quantity is almost proportional to the 1/2 power of time in this empirical formula as shown in Eq. (11):

$$q_t = k_i t^{1/2} + C \quad (11)$$

where k_i (mg/g h^{1/2}) is the intraparticle diffusion rate constant.

2.4.4. Validity of kinetic model

The applicability of a kinetic model can be identified by Δq (%), which is the normalized standard deviation, and expressed as Eq. (12):

$$\Delta q(\%) = 100 \sqrt{\frac{\sum [(q_{exp} - q_{cal})/q_{exp}]^2}{N - 1}} \quad (12)$$

where N is the number of data points, q_{exp} (mg/g) is the experimental adsorption capacity and q_{cal} (mg/g) is the calculated adsorption capacity.

2.5. Thermodynamic study

Thermodynamic parameters such as standard Gibbs free energy change (ΔG°), standard enthalpy change (ΔH°) and standard entropy change (ΔS°) were estimated to evaluate the feasibility and nature of the adsorption process [21]. ΔG° , ΔH° and ΔS° can be calculated from the following equations [13]:

$$\Delta G^\circ = -RT \ln K_L \quad (13)$$

$$\ln K_L = -\frac{\Delta H^\circ}{RT} + \frac{\Delta S^\circ}{R} \quad (14)$$

where R (8.314 J/mol K) is the gas constant and T (K) is the absolute temperature of the solution. K_L (L/mg) is the Langmuir constant.

2.6. Isotheric heat of adsorption

Isotheric heat of adsorption (ΔH_x , kJ/mol) defined as the heat of adsorption determined at constant amount of adsorbate adsorbed is one of the basic requirements for the characterization and optimization of an adsorption process. The magnitude of ΔH_x is calculated by means of the Clausius-Clapeyron equation [22].

$$\frac{d(\ln C_e)}{dT} = -\frac{\Delta H_x}{RT} \quad (15)$$

where C_e (mg/L) is the concentrations of paclitaxel at equilibrium, R (8.314 J/mol K) is the gas constant and T (K) is the absolute temperature of the solution.

3. Results and discussion

3.1. Analysis of adsorption isotherm and equilibrium

The adsorption isotherm describes how the adsorbate molecules distribute between the liquid phase and the solid phase when the adsorption process reaches an equilibrium state. Analysis of the isotherm data by fitting them to different isotherm models is an important step in finding a suitable model that can be used for design purposes [23]. Fig. 2 shows a plot of paclitaxel loading on the adsorbent HP-20 against the paclitaxel equilibrium concentration in the liquid phase at 298, 303 and 308 K. As the initial paclitaxel concentration increased, the amount of paclitaxel adsorbed on HP-20 increased until an equilibrium state. The data for equilibrium adsorption isotherms were fitted into Langmuir, Freundlich, Temkin, and Dubinin-Radushkevich isotherms to investigate the adsorption behavior in detail.

For the Langmuir isotherm, the plot of $1/q_e$ against $1/C_e$ of Eq. (2) should give a linear relationship, from which the Langmuir isotherm parameters K_L and q_{max} can be determined from the slope

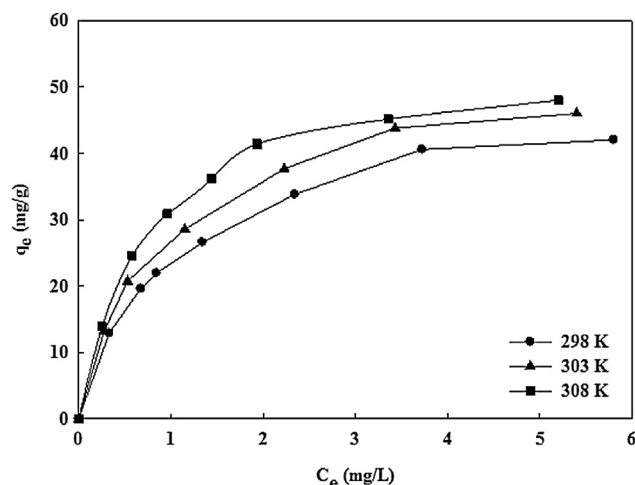


Fig. 2. Adsorption isotherm for paclitaxel onto HP-20 at different temperatures.

and the intercept (figure not shown). The parameters obtained in the isotherm equation, together with a determination coefficient (r^2), are listed in Table 1. The maximum adsorption capacity (q_{max}) varied from 45.46 mg/g to 56.82 mg/g with the range of temperatures studied. The obtained value of q_{max} was much lower than that in the adsorption of echinocandin B from *Aspergillus nidulans* broth using HP-20 (217.86 mg/g at 25 °C) [12] and comparable to that in the adsorption of anthocyanins from black bean wastewater using HP-20 (41.32 mg/g at 25 °C) [24]. The value of q_{max} increased with an increase in temperature, indicating that the adsorption process is endothermic in nature. More adsorption energy is supplied at higher temperatures to enhance the physical binding of an adsorbate in the active site of an adsorbent. Moreover, paclitaxel, which is insoluble in water, has a stronger hydrophobic interaction with an adsorbent rather than that with water molecules. Thus, the maximum adsorption capacity would increase. The essential characteristics of a Langmuir isotherm can be expressed by a dimensionless equilibrium parameter or separation factor, R_L [14]:

$$R_L = \frac{1}{(1 + K_L C_0)} \quad (16)$$

where K_L is the Langmuir constant (L/mg) and C_0 is the initial concentration of paclitaxel (mg/L). The R_L values indicate the type of the isotherm to be either unfavorable ($R_L > 1$), linear ($R_L = 1$), favorable ($0 < R_L < 1$) or irreversible ($R_L = 0$) [25]. The R_L value ranges between 0.329 and 0.348 for the range of temperatures studied (Table 1). An R_L value between 0 and 1 indicates favorable adsorption. The equilibrium data fitted the Langmuir expression with a r^2 value of 0.9930–0.9991.

For the Freundlich isotherm, the plot of $\log q_e$ against $\log C_e$ of Eq. (3) should give a linear relationship, from which $1/n$ and K_F can be determined from the slope and the intercept (figure not shown). The parameters obtained in the isotherm equation, together with a determination coefficient (r^2), are listed in Table 1. The Freundlich constant (K_F) related to adsorption capacity varied from 22.79 mg/g (L/mg)^{1/n} to 29.24 mg/g (L/mg)^{1/n} with the range of temperatures studied. The value of K_F increased with an increase in temperature, indicating that the adsorption process is endothermic in nature. The n value indicates the degree of nonlinearity between solution concentration and adsorption as follows: if $n = 1$, then adsorption is linear; if $n < 1$, then adsorption is a chemical process; if $n > 1$, then adsorption is a physical process. From Table 1, the value of $1/n$ was 0.465, 0.465 and 0.463 at 298, 303 and 308 K, respectively. In other words, the n value in this study was found to be 2.15–2.16 for all investigated temperatures. The situation $n > 1$ is most common and may be due to a distribution of surface sites or any factor that causes

Table 1
Langmuir, Freundlich, Temkin, and Dubinin-Radushkevich isotherm constants for the adsorption of paclitaxel onto HP-20.

Isotherm	Parameter	Temperature (K)		
		298	303	308
Langmuir	q_{\max} (mg/g)	45.46	51.02	56.82
	K_L (L/mg)	1.17	1.26	1.28
	R_L	0.098–0.348	0.092–0.332	0.091–0.329
	r^2	0.9930	0.9969	0.9991
Freundlich	K_F (mg/g (L/mg) ^{1/n})	22.79	25.82	29.24
	1/n	0.465	0.465	0.463
	r^2	0.9910	0.9846	0.9536
Temkin	B (J/mol)	11.39	12.02	12.54
	K_T (L/mg)	8.52	10.43	12.27
	r^2	0.9913	0.9959	0.9921
Dubinin-Radushkevich	q_D (mg/g)	34.76	39.45	42.36
	$K_{DR} \times 10^7$ (mol/J) ²	9	8	7
	E (kJ/mol)	2.36	2.50	2.67
	r^2	0.9054	0.9489	0.9686

a decrease in adsorbent-adsorbate interaction with increasing surface density [26,27]. Values within the range of 1–10 represent favorable adsorption and physical adsorption of paclitaxel onto HP-20 [28–30]. The equilibrium data fitted the Freundlich expression with an r^2 value of 0.9536–0.9910.

The plot of q_e against $\ln C_e$ of Eq. (4) for the Temkin isotherm and the plot of $\ln q_e$ against ε^2 of Eq. (5) for the Dubinin-Radushkevich isotherm should give a linear relationship (figure not shown). The parameters calculated from the slope and intercept in the linear forms of the two isotherms, together with a determination coefficient (r^2), are listed in Table 1. The equilibrium binding constant (K_T) related to the maximum binding energy in the Temkin isotherm was 8.52, 10.43 and 12.27 L/mg. The value of K_T increased with an increase in temperature, confirming that the physical binding capacity between HP-20 and paclitaxel increased as temperature increased in the adsorption process. B , which is a constant related to the heat of adsorption, was 11.39, 12.02 and 12.54 J/mol, values which are lower than 20 J/mol. This result means that there was a physical adsorption process [29]. The theoretical saturation adsorption capacity (q_D) in the Dubinin-Radushkevich isotherm was 34.76, 39.45 and 42.36 mg/g at 298, 303 and 308 K, respectively. E , which is the adsorption energy, was 2.36, 2.50 and 2.67 kJ/mol, values which are lower than 8 kJ/mol. This result also supports the notion that it was a physical adsorption process [25,29]. The equilibrium data fitted both the Temkin and Dubinin-Radushkevich expressions with an r^2 value of 0.9913–0.9959 and 0.9054–0.9686, respectively. Based on these results, it was observed that the highest values of r^2 were in the range between 0.9930 and 0.9991 for the Langmuir isotherm, indicating that the Langmuir adsorption isotherm was the best model for paclitaxel adsorption onto HP-20. The fact that the Langmuir isotherm fits the experimental data very well suggests monolayer coverage of paclitaxel onto HP-20 surface as well as homogeneous distribution of active sites on the HP-20 surface, for the Langmuir isotherm assumes that the surface is homogeneous.

3.2. Analysis of adsorption kinetics

In order to investigate the process of paclitaxel adsorption on HP-20, three kinetic models were used: pseudo-first-order, pseudo-second-order and intraparticle diffusion models. Because the pseudo-first-order and pseudo-second-order models cannot identify a diffusion mechanism, the intraparticle diffusion model was also tested.

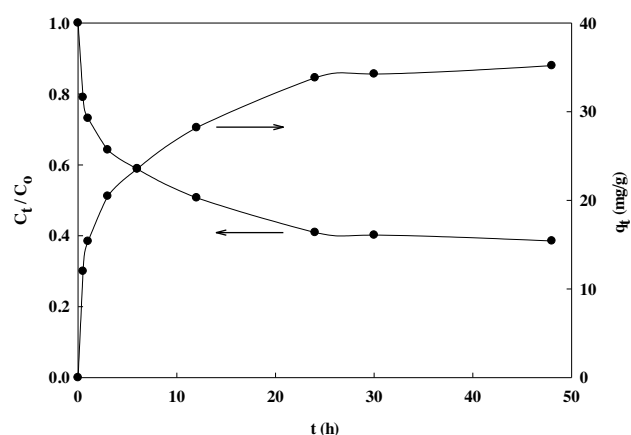


Fig. 3. The variation of solid phase paclitaxel concentrations with time at 298 K. The initial concentration of paclitaxel, weight of adsorbent HP-20, and agitation speed were 5.7 mg/L, 0.1 g/L, and 150 rpm, respectively.

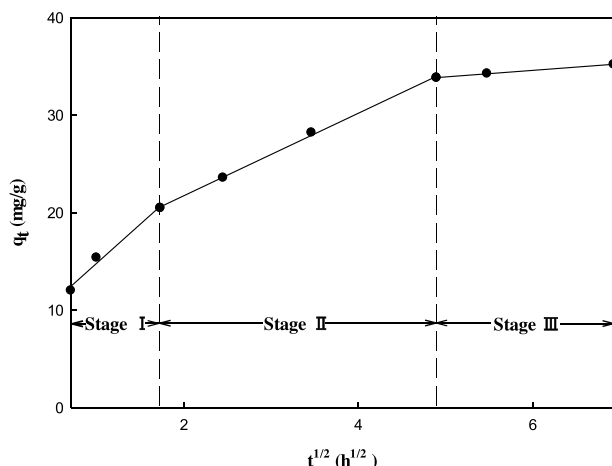
3.2.1. Pseudo-first-order and pseudo-second-order models

A plot of $\ln(q_e - q_t)$ against t of Eq. (9) should give a linear relationship, from which parameters of a pseudo-first-order kinetic model ($q_{e,cal}$, k_1) can be determined from the slope and intercept. The parameters obtained in the pseudo-first-order equation, together with r^2 and Δq , are listed in Table 2. The equilibrium adsorption capacity, q_e , is required to fit the data, but in many cases q_e remains unknown due to slow adsorption processes. For this reason, it is necessary to obtain the real equilibrium adsorption capacity by extrapolating the experimental data to $t = \infty$ or by using a trial and error method [23]. Also, in many cases, the pseudo-first-order kinetic model does not fit well over the whole range of contact time and is generally applicable over the initial stage of adsorption processes [23]. For the pseudo-first-order kinetic model, the obtained Δq value (19.4%) was relatively large and the calculated q_e value ($q_{e,cal}$) was much lower than the experimental q_e value ($q_{e,exp}$) in Table 2. The experimental and calculated values of q_e showed a significant difference. These results indicate that the experimental data do not agree with the pseudo-first-order kinetic model for the adsorption of paclitaxel onto HP-20.

Fig. 3 illustrates the variation of solid phase paclitaxel concentrations with time at 298 K. For the pseudo-second-order kinetic model, the plot of t/q_t against t of Eq. (10) should give a linear relationship, from which q_e and k_2 can be determined from the slope and the intercept (figure not shown). The parameters obtained in the pseudo-second-order equation, together with r^2 and Δq ,

Table 2
Parameters of pseudo-first-order and pseudo-second-order kinetic models for the adsorption of paclitaxel onto HP-20 at 298 K.

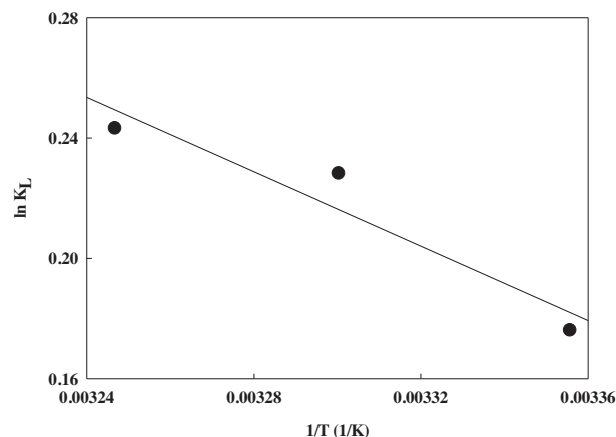
Initial concentration (mg/L)	$q_{e,exp}$ (mg/g)	Pseudo-first-order kinetic model				Pseudo-second-order kinetic model			
		$q_{e,cal}$ (mg/g)	k_{i1} (h^{-1})	r^2	Δq (%)	$q_{e,cal}$ (mg/g)	k_{i2} (g/mg h)	r^2	Δq (%)
5.7	35.2	23.24	0.12	0.99	19.4	36.63	0.012	0.9974	2.5

**Fig. 4.** Intraparticle diffusion plot for adsorption of paclitaxel onto HP-20 at paclitaxel concentration of 5.7 mg/L, HP-20 of 0.1 g/L, and temperature of 298 K. The Stage I, Stage II, and Stage III represent external surface adsorption, intraparticle diffusion, and final equilibrium, respectively.

are listed in Table 2. The higher r^2 value (0.9974) and smaller Δq value (2.5%) of the second-order kinetic model compared to the r^2 value (0.9900) and Δq value (19.4%) of the first-order kinetic model confirm that the second-order kinetic model was a better fit to represent the experimental data. The calculated $q_{e,cal}$ value from the second-order kinetic model also agreed well with the experimental data ($q_{e,exp}$).

3.2.2. Intraparticle diffusion model

The intraparticle diffusion model was applied to determine if the rate-limiting step is intraparticle diffusion. If the mechanism of the adsorption process follows intraparticle diffusion, the plot of q_t versus $t^{1/2}$ would be a straight line and k_i and C can be obtained from the slope and the intercept of the plot. C gives an idea about the thickness of the boundary layer, i. e., the larger the intercept, the greater the boundary layer effect [13,31]. As shown in Fig. 4, the plot was multi-linear and there were three different portions, indicating three different stages in adsorption. The first portion is the instantaneous adsorption or external surface adsorption stage, where paclitaxel migrates through the solution to the exterior surface of the porous HP-20 particles (Stage I). This portion was attributed to bulk diffusion. The second portion is the gradual adsorption stage, where paclitaxel moves within the particles (Stage II). This portion is due to intraparticle diffusion [13]. The third portion is the final equilibrium stage, where the paclitaxel is adsorbed at sites on the interior surface of HP-20 particles (Stage III). In this portion, intraparticle diffusion starts to slow down due to the low paclitaxel concentration remaining in the solution. Generally, the third stage is very rapid and does not constitute a rate-limiting step in the adsorption [23]. Similar adsorption patterns have also been obtained in previous studies [13,23,32]. The values of k_{i1} and k_{i2} were obtained from the slope of the first and second linear portions and the value of C was obtained from the intercept of the second linear portion of the plot. The intraparticle diffusion parameters for the adsorption process are summarized in Table 3. The values of r^2 and Δq for this model were 0.9991 and 3.4%, respectively,

**Fig. 5.** Plot of $\ln K_L$ versus $1/T$.

indicating that the adsorption of paclitaxel onto HP-20 followed the intraparticle diffusion model after 3 h. However, the linear line did not pass through the origin. The deviation of the line from the origin indicates that intraparticle diffusion was not the only rate-limiting step and boundary layer control may be involved in the process [13,33]. Since the value of k_{i1} in bulk diffusion (Stage I) is greater than that of k_{i2} in intraparticle diffusion (Stage II), the latter affected the rate-limiting step more significantly (Table 3). Furthermore, many compounds in the culture broth were adsorbed to the adsorbent, causing a reduction in the pore size of the adsorbent, but paclitaxel would be able to diffuse into the pores of HP-20 (average pore diameter: 24–26 nm), considering the molecular size of paclitaxel ($1.0 \times 1.5 \times 2.0$ nm) based on the space filling model [34].

3.3. Analysis of adsorption thermodynamics

From Eqs. (13) and (14), the thermodynamic parameters including standard Gibbs free energy change (ΔG°), standard enthalpy change (ΔH°) and standard entropy change (ΔS°) were calculated. The plot of $\ln K_L$ against $1/T$ of Eq. (14) should give a linear relationship, from which ΔH° and ΔS° can be determined from the slope and the intercept, as shown in Fig. 5. The thermodynamic parameters of paclitaxel adsorption onto HP-20 are given in Table 4. The value of ΔH° for paclitaxel adsorbed onto HP-20 was +6.59 kJ/mol, indicating that the adsorption was physical in nature, involving weak forces of attraction between the paclitaxel and HP-20. The low value of ΔH° (less than 40 kJ/mol) implies that there was loose bonding between the adsorbate molecules and the adsorbent surface [23,35–37]. In addition, the positive value of ΔH° indicates that the adsorption was also endothermic, thereby demonstrating that this process was stable energetically. The values of ΔG° were found to be -0.39 , -0.58 and -0.62 kJ/mol at 298 K, 303 K and 308 K, respectively. The ΔG° values decreased as the temperature increased, suggesting that adsorption might be more spontaneous at higher temperature. The Gibbs free energy indicates the spontaneity of the adsorption process, where higher negative values reflect a more energetically favorable adsorption process. The negative ΔG° values obtained for all investigated temperatures in this study confirm the feasibility of using the adsorbent and the spontaneity of adsorption. Generally, the change of free energy for

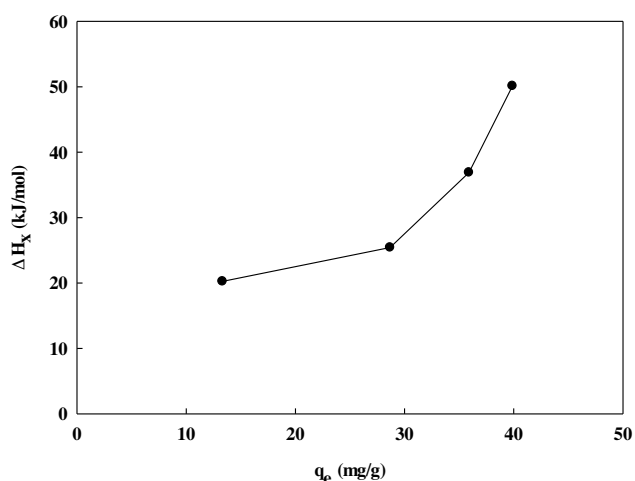


Fig. 6. Plot of isosteric heat of adsorption against surface loading (q_e) for adsorption of paclitaxel onto HP-20.

Table 3
Parameters of intraparticle diffusion model for the adsorption of paclitaxel onto HP-20 at 298 K.

Initial concentration (mg/L)	k_{i1} (mg/g h ^{1/2})	k_{i2} (mg/g h ^{1/2})	C	r ²	Δq (%)
5.7	8.02	4.23	13.26	0.9991	3.4

physical adsorption (physisorption) is between -20 and 0 kJ/mol, while chemical adsorption (chemisorption) is in the range of -80 and 400 kJ/mol [38]. This fact further indicates that the adsorption of paclitaxel onto HP-20 was by physisorption. These results are consistent with the results obtained from the Temkin and Dubinin-Radushkevich isotherms. The value of ΔS° for paclitaxel adsorbed onto HP-20 was $+23.49$ J/mol K. The positive value of ΔS° suggests an increase in the degree of freedom of the adsorbed paclitaxel, indicating that the adsorption was spontaneous in nature. Based on this result, it was demonstrated that water molecules around HP-20 were released during adsorption and paclitaxel was adsorbed to increase the randomness of the entire adsorption system. Furthermore, the positive value of ΔS° suggests high-affinity adsorption involving hydrophobic forces of attraction between the paclitaxel and HP-20 [39]. The values of isosteric heat of adsorption (ΔH_x) were also obtained from the slope of a plot of $\ln C_e$ versus $1/T$ for different amounts of adsorbate onto adsorbent ($q_e = 13, 29, 36, 40$ mg/g). As shown in Fig. 6, the values of ΔH_x were between 20 and 50 kJ/mol indicating that the adsorption of paclitaxel onto HP-20 was a physical process involving weak interactions [22]. Variation in ΔH_x with surface loading (q_e) can be due to adsorbate–adsorbate interaction followed by adsorbate–adsorbent interaction. Initially, at lower q_e values, adsorbate–adsorbate interaction takes place resulting in low ΔH_x values. As q_e increases, adsorbate–adsorbent interaction occurs resulting in high heats of adsorption.

4. Conclusions

The adsorption of the anticancer agent paclitaxel from plant cell cultures onto Diaion HP-20 has been studied in a batch experimental system. The four most common isotherms, namely the Langmuir, Freundlich, Temkin and Dubinin-Radushkevich isotherms, were applied to analyze the adsorption equilibrium experimental data. Based on the Langmuir and Freundlich isotherms, it was found that adsorption capacity increased with an increase in temperature and the adsorption of paclitaxel onto HP-20 was favorable. In the Temkin and Dubinin-Radushkevich

Table 4
Thermodynamic parameters for the adsorption of paclitaxel onto HP-20 at different temperatures.

Temperature (K)	ΔH° (kJ/mol)	ΔS° (J/mol K)	ΔG° (kJ/mol)
298	6.59	23.49	-0.39
303			-0.58
308			-0.62

isotherms, the adsorption of paclitaxel onto HP-20 was a physical process. Comparison of results revealed that the Langmuir model could account for the paclitaxel adsorption equilibrium data, with the highest accuracy among the four adsorption models considered, indicating the monolayer adsorption of paclitaxel onto a homogeneous HP-20 surface. The adsorption kinetics were described well by the pseudo-second-order kinetic model, while intraparticle diffusion was not the only rate-limiting step and boundary layer control may have been involved in the adsorption process. The value of ΔH° for the adsorption process was $+6.59$ kJ/mol, indicating that the adsorption was physical in nature, involving weak forces of attraction between the paclitaxel and HP-20, and tended to be endothermic. The ΔG° values were negative and decreased as the temperature increased. The adsorption was more spontaneous at higher temperatures. The positive value of ΔS° indicates an increased randomness at the solid/liquid interface and hydrophobic interaction between the adsorbate and adsorbent through the adsorption of paclitaxel onto HP-20.

Acknowledgements

This research was supported by Basic Science Research Program through the National Research Foundation of Korea (NRF) funded by the Ministry of Education, Science and Technology (Grant number: 2015016271).

References

- [1] M.C. Wani, H. Taylor, M.E. Wall, P. Coggon, A.T. McPhail, Plant antitumor agents VI. The isolation and structure of taxol, a novel antileukemic and antitumor agent from *Taxus brevifolia*, J. Am. Chem. Soc. 93 (1971) 2325–2327.
- [2] J.H. Kim, Paclitaxel: recovery and purification in commercialization step, Korean J. Biotechnol. Bioeng. 21 (2006) 1–10.
- [3] W.P. McGuire, E.K. Rowinsky, N.B. Rosenheim, F.C. Grumbine, D.S. Ettinger, D.K. Armstrong, R.C. Donehower, Taxol: a unique antineoplastic agent with significant activity in advanced ovarian epithelial neoplasms, Int. J. Gynecol. Obstet. 31 (1990) 298.
- [4] J.R. Hsiao, S.F. Leu, B.M. Huang, Apoptotic mechanism of paclitaxel-induced cell death in human head and neck tumor cell lines, J. Oral Pathol. Med. 38 (2009) 188–197.
- [5] K. Rao, J. Hanuman, C. Alvarez, M. Stoy, J. Juchum, R. Davies, R. Baxley, A new large-scale process for taxol and related taxanes from *Taxus brevifolia*, Pharm. Res. 12 (1995) 1003–1010.
- [6] H.K. Choi, J.S. Son, G.H. Na, S.S. Hong, Y.S. Park, J.Y. Song, Mass production of paclitaxel by plant cell culture, Korean J. Plant Biotechnol. 29 (2002) 59–62.
- [7] E. Baloglu, D.G. Kingston, A new semisynthesis of paclitaxel from baccatin III, J. Nat. Prod. 62 (1999) 1068–1071.
- [8] D.J. Kim, H.N. Chang, Enhanced shikonin production from *Lithospermum erythrorhizon* by in situ extraction and calcium alginate immobilization, Biotechnol. Bioeng. 36 (1990) 460–466.
- [9] J.H. Kim, S.S. Hong, Recovery of paclitaxel from suspension culture medium with hydrophobic resin, Korean J. Biotechnol. Bioeng. 15 (2000) 366–369.
- [10] O.L. Gamborg, R.A. Miller, K. Ojima, Nutrient requirements of suspension cultures of soybean root cells, Exp. Cell Res. 50 (1986) 151–158.
- [11] Y.L. Jeon, J.H. Kim, Precipitation characteristics of paclitaxel in solvent systems with different ion exchange resins, Korean J. Chem. Eng. 30 (2013) 1954–1959.
- [12] S.P. Zou, M. Liu, Q.L. Wang, Y. Xiong, K. Niu, Y.G. Zheng, Y.C. Shen, Preparative separation of echinocandin B from *Aspergillus nidulans* broth using macroporous resin adsorption chromatography, J. Chromatogr. B 978–979 (2015) 111–117.
- [13] Y. Li, C. Zhang, Y. Jing, J. Zhang, Adsorption of malachite green from aqueous solution onto carbon prepared from *Arundo donax* root, J. Hazard. Mater. 150 (2008) 774–782.
- [14] T.W. Weber, R.K. Chakravorti, Pore and solid diffusion models for fixed-bed adsorbers, AIChE J. 20 (1974) 228–238.

- [15] M. Hosseini, S.F.L. Mertens, M. Ghorbani, M.R. Arshadi, Asymmetrical Schiff bases as inhibitors of mild steel corrosion in sulphuric acid media, *Mater. Chem. Phys.* 78 (2003) 800–808.
- [16] A. Günay, E. Arslankaya, İ. Tosun, Lead removal from aqueous solution by natural and pretreated clinoptilolite: adsorption equilibrium and kinetics, *J. Hazard. Mater.* 146 (2007) 362–371.
- [17] A. Dabrowski, Adsorption—from theory to practice, *Adv. Colloid Interface Sci.* 93 (2001) 135–224.
- [18] S. Langergren, B.K. Svenska, Zur theorie der sogenannten adsorption gelöster stoffe, *Vetenskapsakad Handlingar* 24 (1898) 1–39.
- [19] Y.S. Ho, G. McKay, Sorption of dye from aqueous solution by peat, *Chem. Eng. J.* 70 (1998) 115–124.
- [20] W.J. Weber, J.C. Morris, Kinetics of adsorption on carbon from solution, *J. Sanit. Eng. Div. Am. Soc. Civ. Eng.* 89 (1963) 31–59.
- [21] V. Sarin, K.K. Pant, Removal of chromium from industrial waste by using eucalyptus bark, *Bioresour. Technol.* 97 (2006) 15–20.
- [22] S. Chowdhury, R. Mishra, P. Saha, P. Kushwaha, Adsorption thermodynamics, kinetics and isosteric heat of adsorption of malachite green onto chemically modified rice husk, *Desalination* 265 (2011) 159–168.
- [23] M. Doğan, M. Alkan, Ö. Demirbaş, Y. Özdemir, C. Özmetin, Adsorption kinetics of maxilon blue GRL onto sepiolite from aqueous solutions, *Chem. Eng. J.* 124 (2006) 89–101.
- [24] X. Wang, Isolation and Purification of Anthocyanins from Black Bean Wastewater Using Macroporous Resins. M.S. Thesis, Utah State University, United States, 2013.
- [25] P.N. Palanisamy, P. Sivakumar, Adsorption studies of basic red 29 by a nonconventional activated carbon prepared from *Euphorbia antiquorum* L, *Int. J. Chem. Tech. Res.* 1 (2009) 502–510.
- [26] F. Haghseresht, G.Q. Lu, Adsorption characteristics of phenolic compounds onto coal-reject-derived adsorbents, *Energy Fuel* 12 (1998) 1100–1107.
- [27] B.E. Reed, M.R. Matsumoto, Modeling cadmium adsorption by activated carbon using the Langmuir and Freundlich isotherm expressions, *Sep. Sci. Technol.* 28 (1993) 97–106.
- [28] K. Fytianos, E. Voudrias, E. Kokkalis, Sorption-desorption behavior of 2,4-dichlorophenol by marine sediments, *Chemosphere* 40 (2000) 3–6.
- [29] J.J. Lee, Isotherm, kinetic and thermodynamic characteristics for adsorption of congo red by activated carbon, *Korean Chem. Eng. Res.* 53 (2015) 64–70.
- [30] A. Özer, H.B. Pirinççi, The adsorption of Cd(II) ions on sulphuric acid-treated wheat bran, *J. Hazard. Mater.* 137 (2006) 849–855.
- [31] D. Kavitha, C. Namasivayam, Experimental and kinetic studies on methylene blue adsorption by coir pith carbon, *Bioresour. Technol.* 98 (2007) 14–21.
- [32] I.A.W. Tan, A.L. Ahmad, B.H. Hameed, Adsorption of basic dye on high-surface-area activated carbon prepared from coconut husk, *J. Hazard. Mater.* 154 (2008) 337–346.
- [33] V.J.P. Poots, G. McKay, J.J. Healy, Removal of basic dye from effluent using wood as an adsorbent, *J. Water Pollut. Control Fed.* 50 (1978) 926–939.
- [34] H. Hata, S. Saeki, T. Kimura, Y. Sugahara, K. Kuroda, Adsorption of taxol into ordered mesoporous silica with various pore diameters, *Chem. Mater.* 11 (1999) 1110–1119.
- [35] P. Cañizares, M. Carmona, O. Baraza, A. Delgado, M.A. Rodrigo, Adsorption equilibrium of phenol onto chemically modified activated carbon F400, *J. Hazard. Mater.* 131 (2006) 243–248.
- [36] O. Abdelwahab, N.K. Amin, Adsorption of phenol from aqueous solution by *Luffa cylindrica* fibers: kinetics, isotherm and thermodynamic studies, *Egypt. J. Aquat. Res.* 39 (2013) 215–223.
- [37] Q. Yang, M. Gao, Z. Luo, S. Yang, Enhanced removal of bisphenol A from aqueous solution by organo-montmorillonites modified with novel gemini pyridinium surfactants containing long alkyl chain, *Chem. Eng. J.* 285 (2016) 27–38.
- [38] M.J. Jaycock, G.D. Parfitt, *Chemistry of Interfaces*, Ellis Horwood Limited, London, 1981.
- [39] S. Gryc, H. Bianco-peled, Binding of amino acids to smart sorbents: where does hydrophobicity come into play? *Langmuir* 20 (2004) 167–174.